Khazar Journal of Science and Technology Volume 8 №1 2024, 58-77
 DOI: 10.5782/2520-6133.2024.8.1.58

Design and Modeling of Smartphone Controlled Vehicle

Nijat Gasimzade
Khazar University, Baku, Azerbaijan
nicat.qasimzada@khazar.org

Abstract

While many have worked on the transition phases of more popular hybrid aerial vehicle configurations. In this paper, we explore a novel multi-mode hybrid Unmanned Aerial Vehicle (UAV). Due to its expanded flying range and adaptability, hybrid aerial vehicles—which integrates two or more operating configurations—have become more and more widespread. The stages of transition between these modes are reasonably important whether there are two or more flight forms present. Whereas numerous have worked on the early stages of more widely used hybrid aerial vehicle types, in this paper a brand-new multi-mode hybrid unmanned aerial vehicle (UAV) will be investigated. In order to fully exploit the vehicle's propulsion equipment and aerodynamic surfaces in both a horizontal cruising configuration and a vertical hovering configuration, we combine a tailless fixed-wing with a four-wing monocopter. By increasing construction integrity over the whole operational range, this lowers drag and wasteful mass when the aircraft is in motion in both modes. The transformation between the two flight states can be carried out in midair with just its current flying actuators and sensors. Through a ground controller, this vehicle may be operated by an Android device.

Keywords: quadcopter; Aerial robots; system design

1. Introduction

Unmanned aerial vehicle (UAV) system has advanced to the point that there are currently four main categories of configurations: fixed-wing, rotor-wing, flapping-wing, and aerostat. Long-range rapid responses can be provided by fixed-wing arrangements. In crowded situations, rotor-wings are handy. In tiny scale applications (micro-UAVs) (Muller, 2001), restricted or undeveloped flapping wings reach impressive levels of flight efficiency and aerostats have potentially unlimited airborne time. Hybrid UAVs exist somewhere between these, and its main goal is to combine two or more designs in a compatible form. A UAV configuration that has both a gliding and a hovering flight state is advantageous for a variety of

UAV applications. While the latter offers flexibility and mobility to travel through restricted and limited surroundings, the earlier enables faster velocities and a greater reach. For instance, in emergency situations, the UAV would have to be available to float at any stage during the operation and have a quick reaction duration across wide range. For the extraction or transport of supplies or individuals, it may be necessary to fly across mountains, jungles or rivers and lakes. A further instance would be in the delivery industry, where service providers may utilize the greater reach to both cut back on the amount of aerodromes required to handle an area and enable mentioned areas to encompass crowded metropolitan areas where conventional airfield are not available. The combination of a gliding state and a floating state on a individual structure presents a number of substantial construction issues, as attractive as these features may sound. The most fundamental of these is that the propulsion systems and aerodynamic surfaces are not completely exploited in both flight regimes, making present approaches highly functionally inefficient. This happens because floating and gliding have inherently diverse functioning concepts; effective floating relies more on rotating airflow than cruising does, which is why optimal flying is focused on longitudinal airflow. This frequently results in a large amount of single phase exclusive elements that reduce flight efficiency by adding unnecessary weight or by acting as an unnecessary cause of drag. Worse than that, the system's weight and structural intricacy may increase if extra elements are required to carry out the shift between the two states. In order to increase the constructional effectiveness of mixed aircraft, initiatives to minimize single-mode exclusive elements have largely been successful. The V-22 Osprey, utilizes the exact thruster components for both flying and floating flight, is a manned case of it. The concept is a powerful example of a hybrid aircraft even if many of its wing surfaces are still single-mode solely and it needs supplementary systems for its conversion phase. CH-46 Sea Knight acquires nearly three times the engagement radius and double the cruising speed relative to the, its only rotor-winged forerunner, yet maintaining comparable hovering characteristics (Norton and Bill, 2004; Frawley and Gerald, 2002). The lack of an on operator minimizes the necessity to adhere to precise configurations in forward flight and permits a wider mass expenditure for additional elements, which leads to a broader diversity of alternatives to improve constructional efficiency in the context of UAVs. A few instances in comparison to the V-22 Osprey can be seen in Figure 1. Structural efficiency can be defined as a characteristic as of a multi-mode aircraft, and can be mathematically represented as:

$$\frac{A_u}{A_{Tot}} \times 100\%$$

In which A_u is the overall aerodynamically responsive area of the aircraft used in all configurations (including propellers, wings, flaps, etc.) and A_{Tot} is the aerodynamically usable region. A vehicle with a distributed structure utilized in all forms would produce a structural efficiency of 100% compared to a craft with entirely individual mechanisms for each configuration have 0%. In this paper, we investigate configurations that give users rapid, long range functionality in even the most impedimental situations by combining the scope of fixed wings with the flexibility of rotor wings.The QuadRanger by PX4 (PX4 Dev Team, 2020) is one instance of a configuration that fuses the two forms of construction onto a single chassis. Such mixtures have separate thrusters and control mechanisms for each of their flight configurations. Some layouts employ a supplemental actuator to reposition some of the thrusters or control mechanisms throughout a transformation phase, increasing construction efficiency. A prime instance of this is the BirdEyeView FireFly6 (BirdsEyeView Aerobotics, 2021), which uses fewer redundant elements in both flight mode. Even more extreme hybrids such as Google's Project Wing (XCompany, 2021) use their own thrusters and monitoring model to shift between and function in both flight configuration.

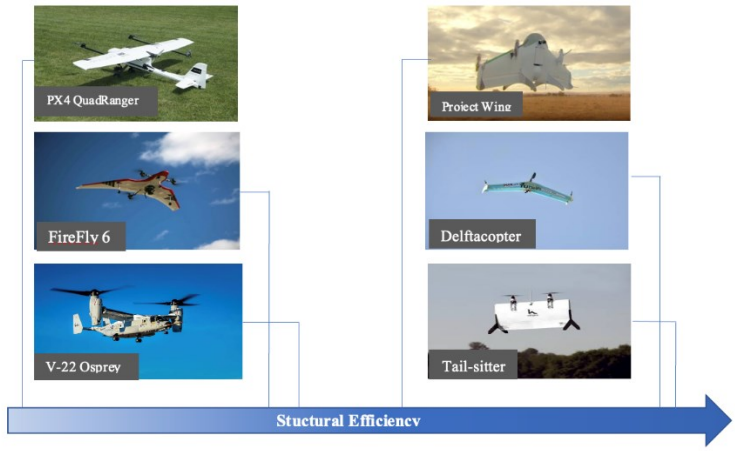

Figure 1. Structural efficiency comparison of various multi-mode aircraft designs

There are designs that achieve even higher compositional performance by using the same operating surfaces and thruster systems for all flight configurations, such as TU Delft's distinctive Delftacopter(De Wagter et al., 2017), which was inspired by biplanes, and ETH Zurich's more straightforward Tail-sitter UAV (Bapst et al., 2015). Even so, the majority of modern hybrid vehicles still use their wing space just for fixed-wing flight. Therefore, to enhance the system performance of the

hybrid and maintain full wing area utilization in both flight configurations, we suggest the fusion of a fixed layout with the monocopter rotor-wing, a craft that rotates its whole fusealage to reach greatly productive flight (Kellas, 2007; Houghton & Hoburg, 2008; Evan et al., 2010; Fregene & Bolden, 2010) contains a list of significant publications on the subject. Because of its demanding handling necessities and entirely spinning structure, the monocopter has originally declined behind other rotor-wing designs. This framework, however, has seen a revival as focus in manned flight has changed to unmanned flight and accurate microelectronic and actuator devices have shrunk in size. It is implemented by hybrid aircraft like Dzyne's ROTORwing (Page & McCue, 2015) for its Vertical Take-Off and Landing (VTOL) phase of flight. But in this design, the despin motor is only used during shift, and the tail arrangement is just involved throughout forward flight.

In order to create a hybrid UAV that is systemically proficient, we initiate the Multimode Hovering Vehicle in this paper as well as its three flight styles, Quadcopter Mode, Fixed Wing Mode, and Monocopter Mode. We define the operational fundamentals and essential concept criteria of such a setup in Section 2, leading to a dynamic model that is described in Section 3.

Monocopters are not a brand-new idea. The samara seed, an achene with wings which uses its whole body to produce lift, is a living instance of how nature has long advocated this theory. The results of research like (Kellas,2007; Lentink et al., 2009) have demonstrated that these seeds have outstanding, passive lift producing characteristics (autorotation), are extremely steady, and can be operated. Because of these desirable qualities, human-made variants included flaps for directional management and propulsion structures to facilitate consistent flight. The Gyroptre, a massive, manned project created by Alphonse Papin and Didier Rouilly (Papin & Rouilly,1915) in the 1910s, serves as an initial illustration of these. Although this prototype didn't take off (both literally and abstractly), it served as the starting point for scientists' efforts to create an aircraft with an effective structural design that can hover. The monocopter idea was revived at the beginning of the twenty-first century. Hoburg and Houghton created a design in 2008 that demonstrated its practicability for usages in enclosed areas by being able to repeatedly fly along a 70 m by 3 m corridor accompanied by a 1.5 m doorway (Houghton & Hobrug, 2008). Additionally, Hoburg and Houghton made two major breakthroughs. The first was the discovery that a propulsion system and flap equipped monocopter can still accomplish passive consistency in hover, returning it to its samara seed predecessors, with the appropriate choice of construction variables. The second involved connecting this naturally influenced configuration to the dynamics and control of helicopters, such as the benefits of employing a fixed angular speed for

the rotor and cyclic motion to achieve forward flight. The monocopter has disadvantages in addition to its incredible systemic efficiency. Specific common and practical payloads, like video cameras, are affected by the continuously revolving fuselage because they are prone to orientation sensitivity. For this kind of payloads, software or supplemental pneumatic parts would be needed to maintain the sensor's direction (Yougren et al., 2009; Hockley & Butka, 2010). The last is heavily reliant on ambient luminance and on-board nutation, while the first results in increased weight and structural difficulty. More importantly, the greater the hover angular speed, the more accurate the detector and regulation would need to be, making both operated and non-actuated workarounds correspondingly more difficult to execute (Consequently, downsizing the configuration presents an increased task).

Nevertheless, these flaws shouldn't be used as an excuse to ignore the concept. There are several payloads that are not vulnerable to revolution, including first aid packages, gas sensors, Global Position Systems (GPS), fertilizers and pesticides, wireless signal relays, to mention a few. In addition, there are devices as spinning Light Detection and Ranging (LIDAR) sensors and event-based cameras that might gain from a regulated rotational movement.

We think that dual-wing monocopters have an exceptionally solid argument within the domain of hybrid UAVs due to their fundamental resemblance to a tailless fixed-wing. We postulate that such a model can have two sections of flying performance inside its operational range as opposed to the single zone of typical hybrid models like the tailsitters because they are able to maintain the wings entirely engaged in both monocopter arrangement and tailless fixed-wing arrangement (Figure 2).

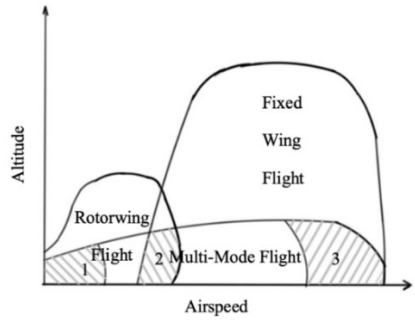

Figure 2. Target efficiency regions of flight of a multi-mode UAV as

The aircraft has 3 operational modes: Quadcopter Mode which has difference from traditional multicopter design by having wings on the arms, Fixed Wing Mode similar to tail-sitter aircrafts, using multiple motors to move forward but main lift

comes from wings enables traveling long distances with relatively low power requirement, Monocopter Mode which is more efficient in take-off and hovering in a specific coordinate. The transition and control process are done by rotating main gear in base of aircraft which arms' gears are in link and rotates wings giving desired angle of attack to aircraft for Monocopter Mode. Wings also contribute to Quadcopter Mode to the lift, making less power usage in motors.

Figure 3. Internal structure of aircraft

The monocopter mode, M-MOD, is an efficient hovering flight mode that spins the entire frame to achieve lift. Aircraft is also capable of transiting to F-MOD, or the fixed wing mode, which is a fixed-wing mode which excels at long endurance and long-distance flights. Staying true to the concept of structural efficiency, aircraft has virtually no redundant surfaces and as all control surfaces and propulsion systems are used in all flight modes. The forward transition phase where aircraft goes from M-MOD to T-MOD would be known as MT-Transition, and the back transition from T-MOD to M-MOD known as TM-Transition. Another motivation for having a particular hovering mode as described above is that due to the rotating nature of UAV to achieve lift, it also has the potential to be capable of entering autorotation in the event of power loss to the propulsion system or merely a way to conserve energy during descent. However, due to this rotating nature of aircraft during F-MOD, the transition phases are more challenging to handle compared to other hybrid UAVs with a more straightforward flight path.

2.1. Propulsion systems contribution

Our propulsion system consists of four identical sets of plastic propellers, brushless direct current motors (BLDC), and electronic speed controllers (ESC). The thrust force generated by the air propelled by the propellers (F_{PM}; F_{SM}) and the torque needed to maintain momentum (τ_{PM}; τ_{SM}) are the other two parts of their dynamic contributions. When simulating the monocopter's propulsion systems, there are two intriguing elements to take into account.

2.2. Communication and Control Systems

There are multiple ways to control the vehicle with a mobile phone: GSM, WI-FI, Bluetooth, IR blaster. The quality of a wireless communication technology is determined by 3 things, distance, speed and power consumption. Only 2 of the 3 specifications can applied at a same time. The range comparison of some wireless communication technology is shown in Figure 4.

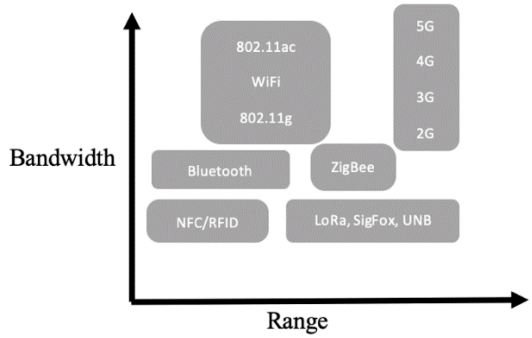

Figure 4. Bandwidth vs Range of wireless technology (Ghayvat et al.,2014].

Each has its own drawbacks and advantages. Determine best solution for application TOPSIS (The Technique for Order of Preference by Similarity to Ideal Solution) method (Hwang and Yoon, 1981; Yoon, 1987; Hwang et al., 1993) is implemented.

Table 1. Decision matrix

Decision Matrix	Range(m)	Impementation hardness	Reliability	User interface	Speed
Weight	0,2	0,15	0,3	0,15	0,2
GSM	35000	2	2	3	1
Wifi	45	3	4	3	4
BLUETOOTH	10	1	2	4	2
IR BLAST	5	1	1	3	4
Application+Rf Module	152	4	5	5	4
Total	35000,3608	5,5678	7,0711	8,2462	7,2801

Next step is vector normalization the decision matrix by given formula:

$$\bar{X}_{ij} = \frac{X_{ij}}{\sqrt{\sum_{j=1}^{n} X_{ij}^2}}$$

Table 2. Vector normalized decision matrix

Vector Normalized Matrix	Range(m)	Impementation hardness	Reliability	User interface	Speed
Weight	0,2	0,15	0,3	0,15	0,2
GSM	0,99999	0,35921	0,28284	0,36380	0,13736
Wifi	0,00129	0,53882	0,56569	0,36380	0,54944
Bluetooth	0,00029	0,17961	0,28284	0,48507	0,27472
IR BLAST	0,00014	0,17961	0,14142	0,36380	0,54944
Application+Rf Module	0,00434	0,71842	0,70711	0,60634	0,54944

Then getting weighted values of each component by multiplying weight of each criteria to each alternatives vector normalized value.

$$t_{ij} = w_j \bar{X}_{ij}$$

Table 3. Weighted normalized decision matrix

Weighted Normalized Matrix	Range(m)	Impementation hardness	Reliability	User interface	Speed
Weight	0,20000	0,05388	0,08485	0,05457	0,02747
GSM	0,00026	0,08082	0,16971	0,05457	0,10989
Wifi	0,00006	0,02694	0,08485	0,07276	0,05494
Bluetooth	0,00003	0,02694	0,04243	0,05457	0,10989
IR BLAST	0,00087	0,10776	0,21213	0,09095	0,10989

In order to find best (A^*) and worst alternative(A^-), maximum value and minimum value is chosen accordingly for beneficial criteria. For cost criteria minimum value is chosen for A^* and maximum value for A^-.

$$A^- = \{< \min(t_{ij} | \, i = 1,2,\dots,m) | \, j \in J^- >, < \max(t_{ij}) \, i = 1,2,\dots,m) | j \in J^+\}$$
$$\equiv \{t_{bj} | j = 1,2,\dots,m\}$$

$$A^* = \{< \max(t_{ij} | \, i = 1,2,\dots,m) | \, j \in J^- >, < \min(t_{ij}) \, i = 1,2,\dots,m) | j \in J^+\}$$
$$\equiv \{t_{wj} | j = 1,2,\dots,m\}$$

Next step is finding distance between the target alternative t_{ij} and the worst condition A^-:

$$S^- = \sqrt{\sum_{j=1}^{n} (t_{ij} - t_{wj})^2}$$

and distance between the target alternative t_{ij} and the best condition A^+:

$$S^+ = \sqrt{\sum_{j=1}^{n} (t_{ij} - t_{bj})^2}$$

Then calculating the similarity to the worst condition:

$$C = \frac{S^-}{(S^+ + S^-)}$$

Alternatives are ranked according to values of these similarities:

Table 4. Ranking alternatives based on similarity to worst condition on weighted normalized decision matrix

Weighted Normalized Matrix	Range	Impemen-tation hardness	Reliability	User interface	Speed	S+	S-	C	Rank
GSM	0,20000	0,05388	0,08485	0,05457	0,02747	0,16498	0,20619	5,00387	2
Wifi	0,00026	0,08082	0,16971	0,05457	0,10989	0,20915	0,16092	-3,33632	5

Bluetooth	0,00006	0,02694	0,08485	0,07276	0,05494	0,25702	0,05372	-0,26423	3
Ir Blast	0,00003	0,02694	0,04243	0,05457	0,10989	0,27685	0,08242	-0,42389	4
Application +Rf Module	0,00087	0,10776	0,21213	0,09095	0,10989	0,19913	0,20844	22,37790	1
A*	0,20000	0,10776	0,21213	0,09095	0,10989				
A-	0,00003	0,02694	0,04243	0,05457	0,02747				

For the speed and range needs of the project, controlling from an application with Bluetooth connection to Ground Control/ Remote Controller is seemed more suitable as it will be able to switch the device even when the vehicle is on the air. Communication scheme is given below:

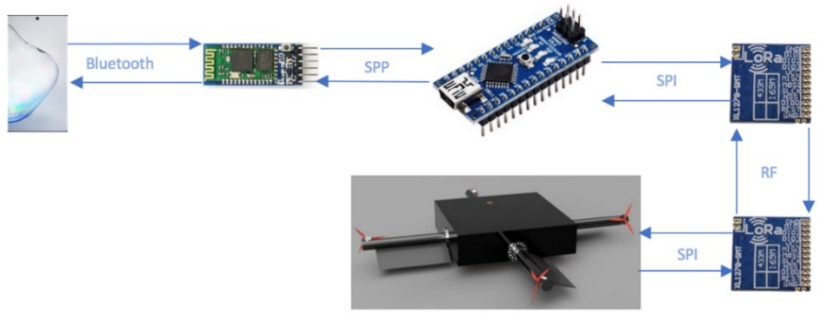

Figure 5. Communication diagram of model.

2.3. Controller Application

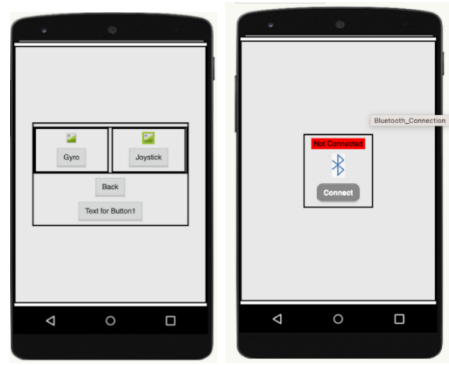

Figure 6. Application's interface

For controller part an android application is designed. In the main page of application, connection to controller over Bluetooth is implemented. After connection is secured, controller selection page is opening where user can choose to control either traditional method “Joystick Mode” or “Gyro Mode”. On “Joystick Mode” there are 2 controller joysticks can be used in all configurations, left one for throttle and yaw motions, right one for pitch and roll motions.

2.3.1. Fuzzy Logic in Controlling

Humans are capable of tremendously adaptable regulation but do not require accurate, quantifiable sensory intake to produce decisions. The astonishing skill of individuals to do a broad range of physiological and cognitive actions without any specific assessments or calculations is a tremendous accomplishment. Instances of commonplace activities include cooking, tuning musical instrument, playing football, parking or adjusting AC. Humans employ their senses of space, time, velocity, shape, temperature and other characteristics of tangible and intangible entities to carry out such routine activities (Pham et al.,2007). Lofti Zadeh developed fuzzy set theory in the middle of the 1960s. In a paper that was published in 1965, Lotfi Zadeh proposed the fuzzy set theory (Zadeh, 1965). From control theory to artificial intelligence, fuzzy logic has been applied to a variety of domains. From compact, simple integrated systems to massive, interconnected workstation-based information collection and regulation structures, fuzzy logic provides an approach for problem-solving operational configurations that adapts itself to execution. The astonishing capacity of humans to use and make sense of information using sensation serves as basis for the concept of fuzzy logic. A systematic framework for rationalization and judgment with ambiguous and imperfect data is offered by rule-based fuzzy logic. It may be put into practice using in software level, hardware level, or a blending of the two. The use of fuzzy logic to solve operational issues simulates human decision-making. The capacity to draw intuitive principles from individual experience and avoid the requirement for a scientific framework of the procedure are the primary upsides of a fuzzy navigation technique. (Yang et al.,2004; Seraii & Howard, 2002).

There are three steps in a fuzzy controller: input, processing, and output. The input step converts inputs from gyro sensors, switches, light detectors, hall sensors and other devices into the proper membership functions and logic values. Every suitable rule is invoked throughout the processing step, producing an outcome for each one before the outcomes are merged. The output step then transforms the merged outcome once again into a particular control output value. The IF-THEN expressions that make up the processing step are composed of a set of logic rules,

with the IF portion serving as the "precursor" and the THEN portion serving as the "resultant". Fuzzy operators like AND, OR, and NOT are used to merge the multiple precursors in fuzzy rule sets. AND utilizes the precursors' lowest possible value, OR uses their peak value, and to provide the "complementary" function NOT deducts a membership function from 1 (Bishop, 1995). Figure 7 illustrates how fuzzy logic is applied to an issue in its entirety. Here, the problem's real-world inputs are represented by the crisp space variables.

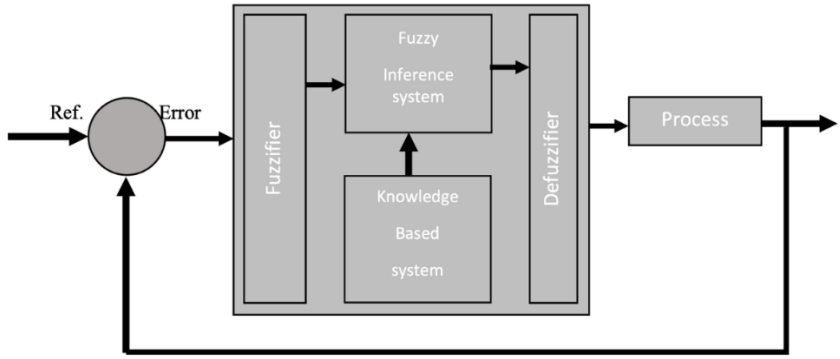

Figure 7. Fuzzy Controller with fuzzy inference system

A fuzzy set's membership function is an extension of the characteristic function in conventional sets. The level of validity is represented in fuzzy logic as an supplement of evaluation. Although degrees of truth and probabilities are sometimes conflated, they are fundamentally different, because fuzzy truth refers to membership in inadequately defined sets rather than the possibility of an occurrence or state. Based on the kinds of changes in the input and output, the membership function may take a wide range of forms. For instance, when defining a acute, crispy value, we use a triangular membership function and when we need a value stays same for some values of variables, a constant value, we use a trapezoidal function, for more complicated relationships gaussian curve can be used. Any function from the given set X to the real unit interval [0, 1] is referred to as a membership function on X. Fuzzy subsets of X are represented by membership functions on X. μA is often used to indicate the membership function that describes a fuzzy set $\bar{A}$. For an element x of X, the membership degree of x in the fuzzy set $\bar{A}$ is the value μA (x). The grade of membership of the element x to the fuzzy set $\bar{A}$ is characterized by the membership degree μA (x). If x doesn't have a membership in fuzzy set membership value is 0; if x is fully a member of the fuzzy set, membership value is 1; if x is fragmentary included in the set, membership value range between 0 and 1.

With the input values collected from LSM6DSO sensor (Figure 8) and maximal working range of motors, input and output fuzzy sets are generated:

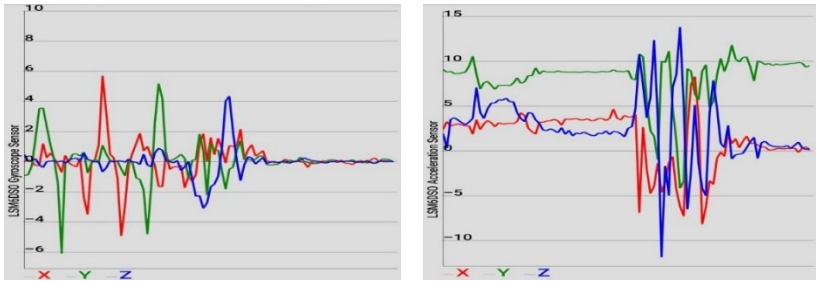

Figure 8. LSM6DSO accelerometer and gyroscope values

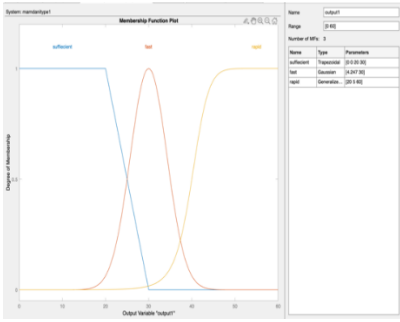

Figure 9. Input Fuzzy

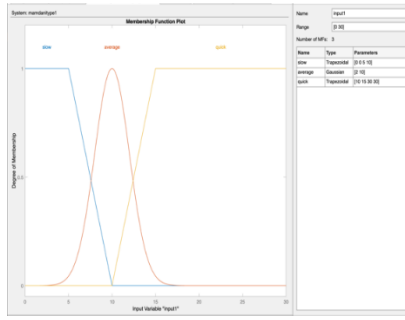

Figure 10. Output Fuzzy Sets

Fuzzy rules are formulated based on human perception. The fuzzy rule base is a set of linguistic rules in the form of "if a set of conditions are satisfied, then a set of consequences are inferred". Based on the above fuzzy subsets, the fuzzy control rules are defined in a general form for three inputs and three outputs fuzzy system shown in Figure 11.

	Rule	Weight	Name
1	If input1 is slow then output1 is suffiecient	1	rule1
2	If input1 is average then output1 is fast	1	rule2
3	If input1 is quick then output1 is rapid	1	rule3

Figure 11. Fuzzy Control Rules

With given values and rules a model is generated on MATLAB software (Figure 12).

Depending on input values, output values are calculated by given rule sets, result of these calculations of some examples are shown in Figure 13, 14, 15.

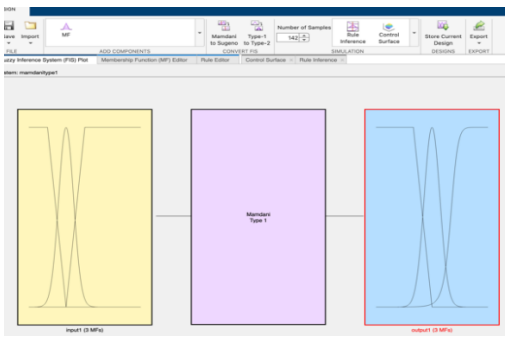

Figure 12. Fuzzy Inference System

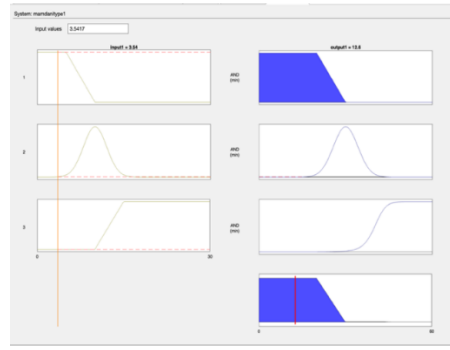

Figure 13. Result of selected random

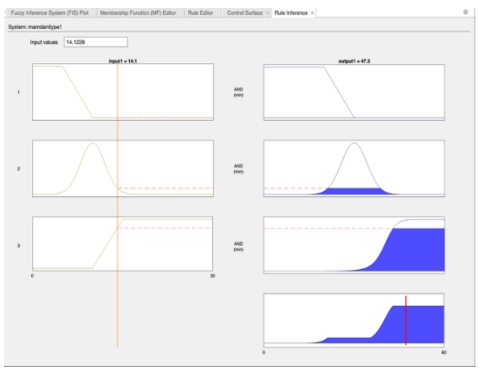

Figure 14. Result of selected random

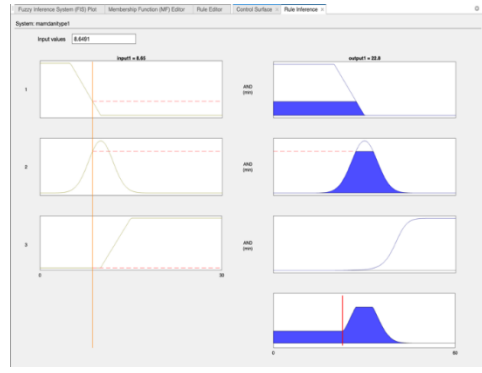

Figure 15. Result of selected random

3. Dynamic Models

The route tuning should be carried out using a dynamic model, which must be generated. The inertial frame XYZ and the corpus frame xyz are both used to establish the source frames.

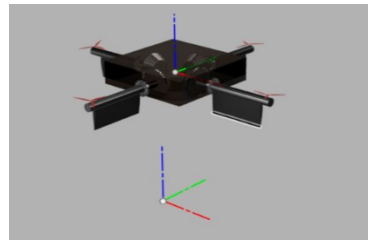

Figure 16. Reference frames

The body frame xyz is attached to the UAV's center of mass with the z-axis coinciding with the yaw axis of M-MOD, and the y-axis coinciding with the yaw axis of F-MOD, with the z axis pointing to M-MOD forward. The frames are illustrated in Figure 17. A free body diagram of aircraft in both F-MOD and MF-Transition are presented in Figures 18 and 19. The orientation of the motors on the wing is characterized to be r_{1m}, r_{2m}, r_{3m}, r_{pm} and r_{4m}, as well as the position of the point of motion of the wing to be $\bar{r}_{1w}$, $\bar{r}_{2w}$, $\bar{r}_{3w}$ and $\bar{r}_{4w}$.

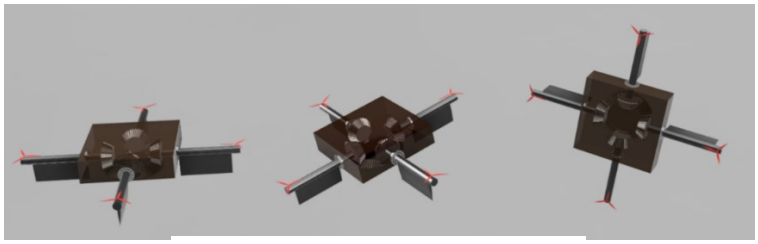

Figure 17. MF-Transition

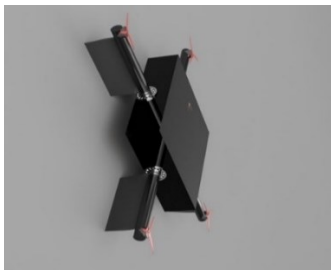

Figure 18. Monocopter Mode

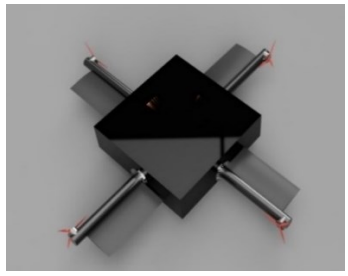

Figure 19. Fixed Wing Mode

The lift and drag forces, $\overline{L_1}$, $\overline{D_1}$, $\overline{L_2}$, $\overline{D_2}$, $\overline{L_3}$, $\overline{D_3}$, $\overline{L_4}$ and $\overline{D_4}$ are also condensed into vectors $\overline{A_{1w}}$, $\overline{A_{2w}}$, $\overline{A_{3w}}$ and $\overline{A_{4w}}$ for each wing as such: $\overline{A_{1w}} = \overline{L_1} + \overline{D_1}$, $\overline{A_{2w}} = \overline{L_2} + \overline{D_2}$, $\overline{A_{3w}} = \overline{L_3} + \overline{D_3}$ and $\overline{A_{4w}} = \overline{L_4} + \overline{D_4}$. The definition of the aerodynamic forces is further elaborated on in Section III-A. W refers to the weight force. The total forces and moments acting on the craft, ∑F and ∑M are formulated as such:

$$\sum \bar{F} = \bar{F_1} + \overline{F_2} + \overline{F_3} + \bar{F_4} + \overline{A_{1w}} + \overline{A_{2w}} + \overline{A_{3w}} + \overline{A_{4w}} + \bar{W}$$

$$\begin{aligned}\sum \bar{M} = {} & \overline{M_1} + \overline{M_2} + \overline{M_3} + \overline{M_4} + \overline{M_{1w}} + \overline{M_{2w}} + \overline{M_{3w}} + \overline{M_{4w}} + \bar{F_1} \times (\bar{r}_{1w}) \\ & + \overline{F_2} \times (\bar{r}_{2w}) + \overline{F_3} \times (\bar{r}_{3w}) + \bar{F_4} \times (\bar{r}_{4w}) + \bar{A} \times (\bar{r}_{1w}) \\ & + \overline{A_2} \times (\bar{r}_{2w}) + \overline{A_3} \times (\bar{r}_{3w}) + \overline{A_4} \times (\bar{r}_{4w})\end{aligned}$$

Aerodynamic Forces and Moments. Using Blade Element Theory (BET) (Leishman, 2006), the overall lift and drag forces for every wing are computed (BET). Each element's aerodynamic forces are represented:

$$dL = c(\alpha_e(\alpha, \delta))v_\infty^2$$

$$dD = d(\alpha_e(\alpha, \delta))v_\infty^2$$

where α is incident angle, flap deflection is δ, α_e is the effective angle of attack, which is a function of previous two, v_∞ is the freestream velocity.

Machine Learning in Stabilization

For flying and stabilizing in certain position the vehicle a lot of calculations are needed to be done. Instead of calculating all the outputs depended on multiple variables machine learning can be used. Machine learning is the science of algorithms that can adapt from practice, consisting of 3 main parts: Input Layer, Hidden Layer and Output Layer (Figure 19). Effectiveness increases as a machine learning system gains more expertise, often in the type of interpretative material or encounters with the surrounding. Every method has a model at its core that explains how features may be converted into an estimation of the objective. A weighted sum of the attributes may be used to indicate the expected value of the goal (motor speed and angle) under the expectation of linearity.

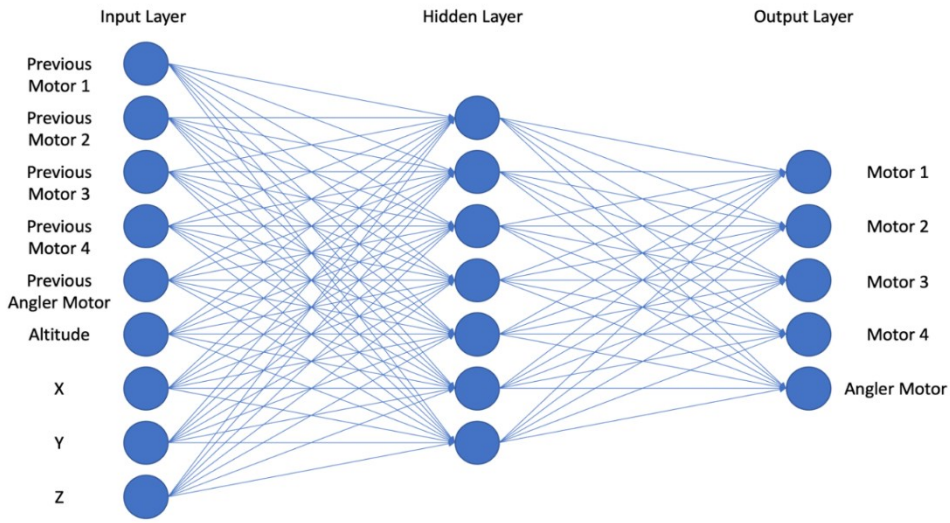

Figure 19. Neural Network for Stabilization

Linear Regression is implemented by plotting a straight line approximately fits best to given data set. Input values are used to get output value with given formula:

$$M_1 = PM_1 \times \omega_{PM1} + PM_2 \times \omega_{PM2} + PM_3 \times \omega_{PM3} + PM_4 \times \omega_{PM4} + PA \times \omega_A + D_A \times \omega_A + D_X \times \omega_X + D_Y \times \omega_Y + D_Z \times \omega_Z + b$$

$$M_2 = PM_1 \times \omega_{PM1} + PM_2 \times \omega_{PM2} + PM_3 \times \omega_{PM3} + PM_4 \times \omega_{PM4} + PA \times \omega_A + D_A \times \omega_A + D_X \times \omega_X + D_Y \times \omega_Y + D_Z \times \omega_Z + b$$

$$M_3 = PM_1 \times \omega_{PM1} + PM_2 \times \omega_{PM2} + PM_3 \times \omega_{PM3} + PM_4 \times \omega_{PM4} + PA \times \omega_A + D_A \times \omega_A + D_X \times \omega_X + D_Y \times \omega_Y + D_Z \times \omega_Z + b$$

$$M_4 = PM_1 \times \omega_{PM1} + PM_2 \times \omega_{PM2} + PM_3 \times \omega_{PM3} + PM_4 \times \omega_{PM4} + PA \times \omega_A + D_A \times \omega_A + D_X \times \omega_X + D_Y \times \omega_Y + D_Z \times \omega_Z + b$$

$$A = PM_1 \times \omega_{PM1} + PM_2 \times \omega_{PM2} + PM_3 \times \omega_{PM3} + PM_4 \times \omega_{PM4} + PA \times \omega_A + A \times \omega_A + D_X \times \omega_X + D_Y \times \omega_Y + D_Z \times \omega_Z + b$$

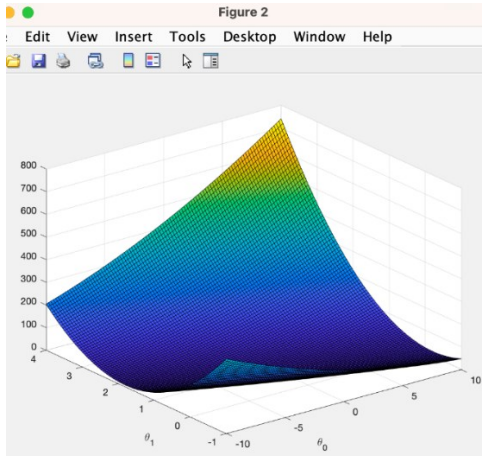

Figure 20. J(θ) dependance from θ_0 and θ_1 in MATLAB

Adjusting the weights is essential part of the system. It is done by cost function which represents error between actual value and predicted value. In other words, it determines how well model is predicting for the given dataset, value of cost function is inversely proportional with accuracy of model.

$$J(\theta) = \frac{1}{2m}\sum_{i=1}^{m}(y_i - \hat{y}_i)^2$$

J(θ) is cost, m is number of examples, y is output values of system, ŷ is predicted values of outputs by model (M_1, M_2, M_3, M_4, A). The objective of linear regression is to minimize the cost function. Reducing the error by updating the parameters (θ) in the direction that incrementally lowers the loss function. One of the popular algorithms used is gradient descent.

$$\theta := \theta - \alpha \frac{\partial J}{\partial \theta}$$

Conclusion

In this paper, we offer a hybrid aircraft prototype system that uses the same aerodynamic surfaces and thruster components for quadcopter, fixed-wing, and rotor-wing flying in order to achieve optimum operational performance. We provide a model that enables the coexistence and complementarity of these structures within the same platform without the installation of any extra or specific mode-only components. Our method takes advantage of mechanical construction factors to both compensate for the specific flying circumstances of the vehicle and to reduce the stability issue of both flight phases. We think the method provides compelling rationale for creating new evaluation and operating techniques that would be useful for applications other than this specific craft considering that the vehicle incorporates principles from two distinct domains of aerodynamics. Our present exploration is concentrated on a number of areas, including further confirmation and enhancements to the model of the platform's dynamics, the implementation of a more complex controller for all flight configurations and the switchover phase, the implementation of extra design parameters that enhance the craft's reaction to user instructions, modifying gyroscope-based guidance, and ultimately enhancing rotorcraft stability.

We think that these initiatives have cleared the way in a variety of disciplines going ahead. First off, we now think we have enough data to create figures of merit to accurately set side by side this system with other comparable hybrid systems. Although the decreased throttle in various flyer configurations is a positive sign, much more research is required to accurately assess the energy efficiency of this hybrid. This can include particular wing configurations according to the objectives the vehicle is meant to perform. The methods of stabilization, controls, and communication should be researched further to be enhanced and supplied with more data. Mechanical design changes are needed to compensate for the vehicle's shortcomings, such as the incapacity to install stationary sensors. This area will be subject of future research.

Reference

Bapst, R., Ritz, R., Meier, L. & Pollefeys, M. (2015). "Design and implementation of an unmanned tail-sitter," in Intelligent Robots and Systems (IROS), 2015 IEEE/RSJ International Conference on. IEEE, pp. 1885–1890.

Birdseyeview aerobotics. (2021). "Welcome to the revolution," https://www.birdseyeview.aero/. (Closed permanently)

Bishop, C. M. (1995). Neural networks for pattern recognition. Oxford, UK: Oxford University Press.

De Wagter, C., Ruijsink, R., Smeur, E., van Hecke, K., Tienen, F., van der Horst, E., & Remes, B. (2017). "Design, control and visual navigation of the delftacopter," arXiv preprint arXiv:1701.00860

Duc Truong Pham, Ashraf Afify, Ebubekir Koc. (2007). Manufacturing cell formation using the Bees Algorithm. IPROMS 2007 Innovative Production Machines and Systems Virtual Conference, Cardiff, UK.

Evan, D. J. P., Ulrich, R., & Humbert, J.S. (2010). "From falling to flying: the path to powered flight of a robotic samara nano air vehicle," Bioinspiration & Biomimetics, vol. 5, no. 4, p. 045009.

Frawley & Gerald. (2002). The International Directory of Military Aircraft, Aerospace Publications (Fyshwick, ACT, Australia

Fregene, K., & Bolden, C.L. (2010). "Dynamics and control of a biomimetic single-wing nano air vehicle," in Proc. IEEE ACC '10, Baltimore, MD, pp. 51–56.

Ghayvat, H., Nag, A., Suryadevara, N., Mukhopadhyay, S.C., Gui, Xiang & Liu, J. (2014). Sharing Research Experiences of Wsn Based Smart Home. International Journal on Smart Sensing and Intelligent Systems. 7.

Hockley, C., & Butka, B. (2010). "The samareye: A biologically inspired autonomous vehcile", in Proc. 29th Digital Avionics Systems Conference Salt Lake City, Utah, pp. 5-C.

Houghton, J., & Hobrug, W. (2008). Fly-by-wire control of a monocopter, experimental projects II technical report, Massachusetts Institute of Technology, Boston, Massachusetts.

Houghton, J., & Hoburg, W. (2008). "Fly-by-wire control of a monocopter," Massachusetts Institute of Technology, Boston, MA, Experimental Projects II Tech. Rep.

Hwang, C.L., Lai, Y.J. & Liu, T.Y. (1993). "A new approach for multiple objective decision making". Computers and Operational Research. 20 (8): 889–899

Hwang, C.L., & Yoon, K. (1981). "Multiple Attribute Decision Making: Methods and Applications" New-York: Springer-Verlag

Kellas, A. (2007). "The guided samara: Design and development of a controllable single-bladed autorotating vehicle", Thesis, Department of Aeronautics and Astronautics, Massachusetts Institute of Technology, Boston, Massachusetts

Leishman, G. J. (2006). Principles of helicopter aerodynamics with CD extra. Cambridge university press

Lentink, D., Dickson, W.B., van Leeuwen, J.L. & Dickinson, M.H. (2009). Leading-edge vortices elevate lift of autorotating plant seeds, Science 324(5933), 1438–1440, American Association for the Advancement of Science, Washington, D.C.

Mark Allan Page, R. A. G. & Matthew Robert McCue. (2015). "Long endurance vertical takeoff and landing aircraft," U.S. Patent 8 991 751.

Mueller, T.J. (2001). Fixed and Flapping Wing Aerodynamics for Micro Air Vehicle Applications, ser. Progress in Astronautics and Aeronautics. Reston, VA: American Institute of Aeronautics and Astronautics, Inc, vol. 195.

Norton & Bill. (2004). Bell Boeing V-22 Osprey, Tiltrotor Tactical Transport, Midland Publishing, Earl Shilton, Leicester, UK

Papin, A., & Rouilly, D. (1915). "Helicopter", U.S. Patent 1 133 660

Pixhawk. (2021) "Ranger quadplane (pixhawk) px4 user guide", Pixhawk, https://docs.px4.io/en/frames_vtol/vtol_quadplane_volantex_ranger_ex_pixhawk.html

Seraji, H. & Howard A. (2002). Behavior-based robot navigation on challenging terrain: A fuzzy logic approach, IEEE Transactions on Robotics and Automation, 18(3), 2002, 308-321.

Youngren, H., Jameson, S., & Satterfield, B. (2009). in Design of the SAMARAI monowing rotorcraft nano air vehicle, in Proc. American Helicopter Society 65th Annual Forum, Grapevine, Texas, pp. 684–697.

Wietzsche, A. (2023). "UAVs in environmental surveillance." Unpublished manuscript.

Xcompany. (2021). "Transforming the way goods are transported", X.Company, https://x.company/projects/wing/

Yang S. X., Li H., Meng M.Q.H. & Liu P.X. (2004) An embedded fuzzy controller for a behaviour-based mobile robot with guaranteed performance, IEEE Transactions on Fuzzy Systems, 12(4), 436-446.

Yoon, K. (1987). "A reconciliation among discrete compromise situations". Journal of the Operational Research Society. 38 (3): 277–286. Doi:10.1057/jors.1987.44

Zadeh, L. (1965) Fuzzy sets, Information and Control, 8(3), 338-353.